INTERNATIONAL JOURNAL FOR NUMERICAL METHODS IN FLUIDS, VOL. 22, 799–810 (1996)

# COMPUTATIONAL STUDIES OF IMPINGING JETS USING $k$–$\varepsilon$ TURBULENCE MODELS

K. KNOWLES

*Aeromechanical Systems Group, Royal Military College of Science, Cranfield University, Shrivenham, Swindon, Wiltshire SN6 8LA, U.K.*

SUMMARY

This paper reports numerical modelling of impinging jet flows using Rodi and Malin corrections to the $k$–$\varepsilon$ turbulence model, carried out using the PHOENICS finite volume code. Axisymmetric calculations were performed on single round free jets and impinging jets and the effects of pressure ratio, height and nozzle exit velocity profile were investigated numerically. It was found that both the Rodi and Malin corrections tend to improve the prediction of the hydrodynamic field of free and impinging jets but still leave significant errors in the predicted wall jet growth. These numerical experiments suggest that conditions before impingement significantly affect radial wall jet development, primarily by changing the wall jet's initial thickness.

KEY WORDS: jets; jet impingement; turbulence; $k$-$\varepsilon$ model; finite volume method

## 1. INTRODUCTION

Impinging jet flows occur under a wide variety of circumstances of practical interest and have consequently received considerable attention in the past.[1–3] Numerical predictions of such flows, however, have been limited in accuracy partly by the performance of turbulence models (which have been developed for flows parallel to walls). As Launder[4] has pointed out, computational facilities are now available for economic solutions of elliptic (rather than parabolic) flows. Consequently, impinging jets are receiving renewed attention.[4]

In our earlier work in impinging jets in cross-flow[5] it was argued that a simple $k$–$\varepsilon$ model was sufficient for the low nozzle hights (and therefore short free jet lengths) of interest. At the same time there is no consensus on which turbulence model performs best for such flows. Jones and McGuirk[6] modelled a round turbulent jet in cross-flow using a three-dimensional coarse grid. It was found that using such a grid together with a simple solver procedure made it difficult to assess the $k$–$\varepsilon$ turbulence model used. Childs and Nixon[7] predicted some features of impinging jets from nozzles at various heights above the surface using three-dimensional grids in conjunction with a standard $k$–$\varepsilon$ model. It was found that the jet spreading rate was overpredicted and a reversed flow upstream of the impingement point was observed. Barata *et al.*[8] predicted the hydrodynamic features of a jet in cross-flow using the QUICK solver procedure with a standard $k$–$\varepsilon$ turbulence model. Their main finding was the shortcoming of the turbulence model to predict the shear stress distribution in the impingement zone. Glynn and Jal[2] modelled a single round impinging jet using the $k$–$\varepsilon$ model with Rodi[9] and Malin[10] corrections for the free jet and wall jet respectively. They showed that the Rodi correction gave good agreement with published experimental data for free jets but that the combined modifications, whilst improving the wall jet prediction, still gave too low a spreading rate, with too high an initial wall jet thickness. They only considered one nozzle height above the ground ($h/d_n = 8{\cdot}5$). Glynn and Jal also calculated the effect of

CCC 0271–2091/96/080799–12

*Received March 1994*
*Revised August 1995*

different nozzle pressure ratios on the free jet spreading rate; they found that increasing pressure ratio caused an increase in free jet spreading, in contrast with the experimental evidence (see Section 3.1). Van Dalsem *et al.*[11] predicted the ground vortex formed by a single jet in cross-flow using a simple Baldwin–Lomax algebraic turbulence model. They predicted ground plane pressure distributions and found them to agree reasonably with experimental results. They also conducted some preliminary modelling of elliptical nozzles and unsteady flow effects.

Knowles and Bray's[5] initial computational work used the $k$–$\varepsilon$ turbulence model (with standard constant values) to model single-nozzle parametric trends (effect of pressure ratio, height, cross-flow velocity ratio and ground plane motion). This work identified which flow field parametric trends were not adequately captured by the model and suggested where the shortcomings might lie. In particular, the effect of nozzle height on wall jet penetration into cross-flow and the reduction of this penetration with moving ground plane operation were both felt to be poorly predicted because of the simple turbulence model used. With this in mind, we present here a study of the effect of some modifications to the $k$–$\varepsilon$ model on impinging jet flow fields. Cross-flow is not considered at this stage.

This paper reports numerical modelling of jets using the PHOENICS finite volume code. This has been used to investigate the effects of pressure ratio, nozzle height, nozzle exit conditions and turbulence model on the flow field of free and impinging jets. The turbulence modelling used the standard $k$–$\varepsilon$ model as well as the Rodi[9] and Malin[10] corrections to this.

## 2. MATHEMATICAL FORMULATION

The mean governing equations for single-phase, three-dimensional, steady state flow are given by

$$\frac{\partial(\rho U)}{\partial x}+\frac{\partial(\rho V)}{\partial y}+\frac{\partial(\rho W)}{\partial z}=0, \tag{1}$$

$$\frac{\partial(\rho U\phi)}{\partial x}+\frac{\partial(\rho V\phi)}{\partial y}+\frac{\partial(\rho W\phi)}{\partial z}=\frac{\partial}{\partial x}\left(\Gamma_\phi\frac{\partial\phi}{\partial x}-\rho\overline{u\phi}\right)+\frac{\partial}{\partial y}\left(\Gamma_\phi\frac{\partial\phi}{\partial y}-\rho\overline{v\phi}\right)+\frac{\partial}{\partial z}\left(\Gamma_\phi\frac{\partial\phi}{\partial z}-\rho\overline{w\phi}\right)+S_\phi, \tag{2}$$

where $\phi$ is the dependent variable, $\rho$ is the density, $U$, $V$ and $W$ are the velocity components, $\Gamma_\phi$ is the diffusion coefficient for the dependent variable in question and $S_\phi$ is the corresponding source of $\phi$ per unit volume. Terms such as $\rho\overline{u\phi}$ represent the shear stresses and additional equations are needed to model them. Turbulence modelling was obtained by using the standard $k$–$\varepsilon$ model and modified versions of this.

The standard $k$–$\varepsilon$ model used in the present study is that built into the PHOENICS code which determines the Reynolds stresses through the use of the Boussinesq eddy viscosity concept, given by

$$-\rho\overline{u_iu_j}=\rho\nu_t(U_{ij}+U_{ji})-\tfrac{2}{3}\rho k\delta_{ij}. \tag{3}$$

The eddy viscosity $\nu_t$ is found from $\nu_t=C_\mu C_D k^2/\varepsilon$, where $k$ and $\varepsilon$ are the turbulent kinetic energy and its rate of dissipation respectively. The two transport equations used for the solutions of $k$ and $\varepsilon$ are given by

$$(\rho k)_t+\left(\rho U_i k-\rho\frac{\nu_t}{\sigma_k}k_i\right)_i=\rho(P_k-\varepsilon), \tag{4}$$

$$(\rho\varepsilon)_t+\left(\rho U_i\varepsilon-\rho\frac{\nu_t}{\sigma_\varepsilon}\varepsilon_i\right)_i=\rho\frac{\varepsilon}{k}(C_{1\varepsilon}P_k-C_{2\varepsilon}\varepsilon), \tag{5}$$

where $P_k = -u_i u_j U_{ij}$ is the volumetric production rate of kinetic energy and the standard values of the unmodified empirical constants are $C_\mu C_D = 0{\cdot}09$, $C_{1\varepsilon} = 1{\cdot}44$, $C_{2\varepsilon} = 1{\cdot}92$, $\sigma_k = 1{\cdot}0$ and $\sigma_\varepsilon = 1{\cdot}314$. Previous experience with these standard values indicates that they tend to be less satisfactory for flows such as axisymmetric and wall jets. Rodi[9] suggested a remedy for this, based on making these constants some function of a mean flow retardation parameter, for the prediction of free jets, while Malin[10] suggested a similar remedy for radial wall jets.

The modified $k$–$\varepsilon$ turbulence models employed in the present work involve the use of the Rodi correction for the free jet modelling and the Malin correction for the wall jet. Rodi's correction is given as

$$C_\mu = 0{\cdot}09 - 0{\cdot}04f, \tag{6}$$

$$C_{2\varepsilon} = 1{\cdot}92 - 0{\cdot}0667f. \tag{7}$$

By contrast the Malin correction is

$$C_\mu C_D = 0{\cdot}09, \tag{8}$$

$$C_{2\varepsilon} = 1{\cdot}92 + 0{\cdot}16f. \tag{9}$$

For the free jet $f$ is the mean flow retardation parameter given by

$$f = \left(\frac{b}{W_{max}}\left|\frac{\partial W_{max}}{\partial z}\right|\right)^{0{\cdot}2}, \tag{10}$$

where $W_{max}$ is the maximum velocity at the jet centreline and $b$ is the radial width of the jet. A similar expression is used to calculate $f$ for the wall jet. It should be noted that the formulation of the Malin correction given in equation (9) follows the practice of Glynn and Jal,[2] who quote Malin as their source. Malin himself,[10] however, does not quote his modification explicitly in this form.

Implementation of these corrections for an impinging jet flow field needs care. The process used here follows the practice of Glynn and Jal.[2] A small box is defined around the impingement region, with a diagonal line extending from its upper corner towards the outer corner of the computational domain. Inside the box the standard $k$–$\varepsilon$ model is always applied. When the Rodi correction is used, it is applied to the region between the diagonal line and the jet centreline. Similarly, when the Malin correction is used, it is applied below the diagonal line.

Adjacent to the wall the model of turbulence must account for the viscous effects; to do that, the wall function is used in the present investigation. The wall function may be written as

$$V^+ = \frac{1}{K}\ln(Ez^+), \tag{11}$$

$$k_w = V_\tau^2 (C_\mu C_D)^{-1/2}, \tag{12}$$

$$\varepsilon_w = \frac{V_\tau^3}{Kz}, \tag{13}$$

where $V^+ = V/V_\tau$, $V_\tau = (\tau_w/\rho)^{0{\cdot}5}$, $z^+ = V_\tau z/v_l$, $K = 0{\cdot}435$, $E = 0{\cdot}0$ and $v_l$ is the laminar kinematic viscosity.

The flow equations were solved using an elliptical computer procedure throughout the present work, except for the free jet where a parabolic procedure was used. Compressibility effects were also taken into account. PHOENICS provides two approaches for the modelling of compressible flow: the isentropic flow equation approach and the perfect gas equation approach. In the present work the

latter is used owing to the different total pressures of the jet and ambient air. That is, the density is calculated from the ideal gas law as

$$\rho = p/RT, \tag{14}$$

with the static temperature $T$ coming from the solved-for specific enthalpy using

$$T = h/c_p. \tag{15}$$

## 3. RESULTS AND DISCUSSION

The procedure adopted for modelling the impinging jet consisted basically of first modelling the free jet characteristics using the standard $k$–$\varepsilon$ model as well as the modified version. The calculations were then extended to include impingement. The effect of nozzle exit turbulence intensity was considered in both cases. For the free jet calculations the influence of nozzle exit velocity profile was also investigated.

### *3.1. Free jet*

In the course of the free jet modelling, only half of the jet was modelled owing to its axisymmetry. A grid of 24 × 31 ($y \times z$) was used. Such a grid was found by Knowles and Bray[5] to give an acceptable trade-off of accuracy against computational time. The grid was finest in those parts where property gradients would be expected to be greatest. The two-dimensional grid was a polar co-ordinate system, with the $z$-axis acting as the jet centreline. The $y$-axis was selected as being radial and the $x$-axis defined the angular dimension.

The numerical results were obtained for various nozzle pressure ratios, in the range from 1·05 to 3, and various nozzle exit turbulence intensities, in the range from 1 per cent to 15 per cent. Furthermore, the flow field was calculated using either a uniform velocity profile or some prescribed velocity profile at the exit of the nozzle.

Figures 1 and 2 show the predicted velocity profiles using standard and modified $k$–$\varepsilon$ turbulence models compared with the experimental results of Donaldson and Snedeker[12] at two downstream locations ($z/d_n = 1{\cdot}96$ and 3·92) for turbulence intensities of 5 per cent and 10 per cent. It can be seen that the standard model tends to overpredict the spreading of the jet for all turbulence intensities used, while the Rodi correction improves the predicted results compared with the experiment. Figure 1 also indicates clearly that both models tend to predict fully developed velocity profiles, whereas the experimental results show a potential core of width approximately $0{\cdot}7r_5$ at $z/d_n = 1{\cdot}96$, reducing to approximately $0{\cdot}3r_5$ by $z/d_n = 3{\cdot}92$. The effect of turbulence intensity (at the nozzle exit) on the predicted axial velocity decay is shown in Figure 3. Both versions of the $k$–$\varepsilon$ model tend to overpredict the velocity decay rate, but the prediction is improved as the turbulence intensity is reduced from 10 per cent to 1 per cent or by using the modified version of the model. The effect of turbulence intensity on the rate of decay of the axial velocity is well illustrated in Figure 4 (using the standard $k$–$\varepsilon$ model) with $pr_n = 1{\cdot}1$ and a uniform velocity profile at the exit. The figure shows that as the turbulence intensity is increased from 1·5 per cent to 15 per cent, the rate of decay of the jet as well as the spreading rate is increased. The potential core of the jet is made shorter as the mixing region is diffused in the core. When a parabolic velocity profile is assumed at the exit of the nozzle, the rate of decay of the velocy is increased further, as seen in Figure 5. This is apparently due to the absence of a potential core in the case of the parabolic exit velocity profile.

Increasing the pressure ratio from 1·1 to 2·5 and 3 tends to preserve the jet and increase its width, as can be seen from Figures 6 and 7. This observation tends to agree with the experimental findings of Curtis[13] and to disagree with the PHOENICS predictions of Glynn and Jal.[2] The notable difference for the high-pressure-ratio cases is the presence of peaks at either side of the jet exit plane which are formed

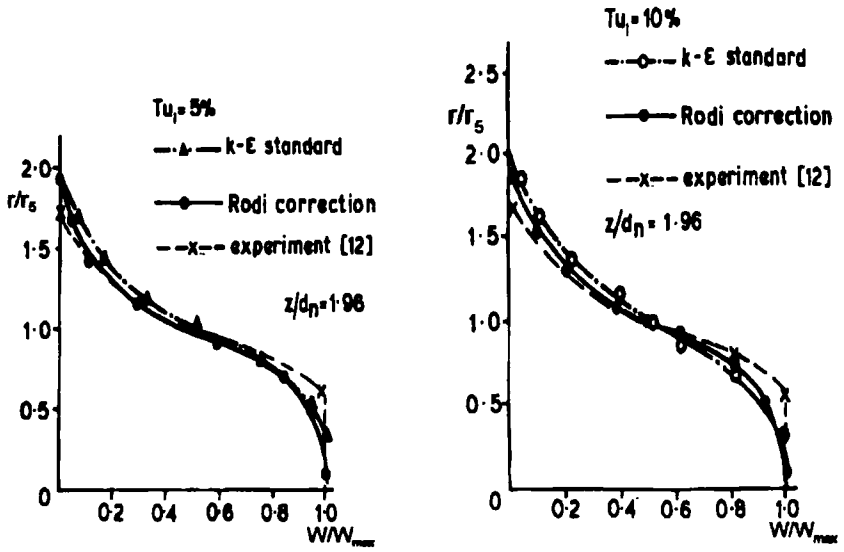


Figure 1. Normalized subsonic free jet velocity profiles at $z/d_n = 1{\cdot}96$

in the vicinity of the nozzle exit. These peaks are due to the high velocity reached as the underexpanded nozzle flow expands to ambient conditions.

### *3.2. Impinging jet*

The impinging jet system modelled in these studies consists of an axisymmetric air jet impinging on a plane normal to its axis at a distance $h$ from the nozzle (see Figure 8). The numerical modelling of this case is an extension of the free jet modelling. A polar, axisymmetric co-ordinate system was used which consisted of 39 cells of total length 0·6177 m in the (radial) $y$-direction. The axial $z$-direction depended on the height of the nozzle above the ground. An elliptical solution of the flow equations is employed

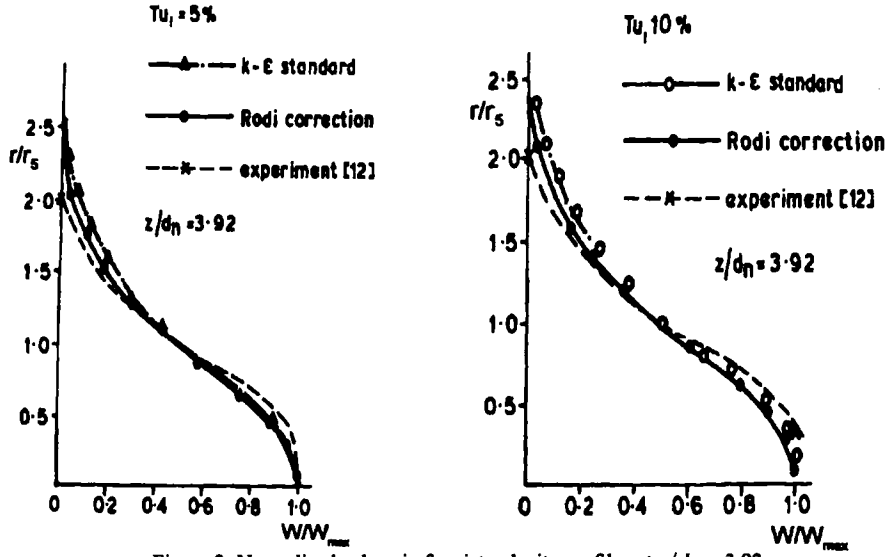


Figure 2. Normalized subsonic free jet velocity profiles at $z/d_n = 3{\cdot}92$

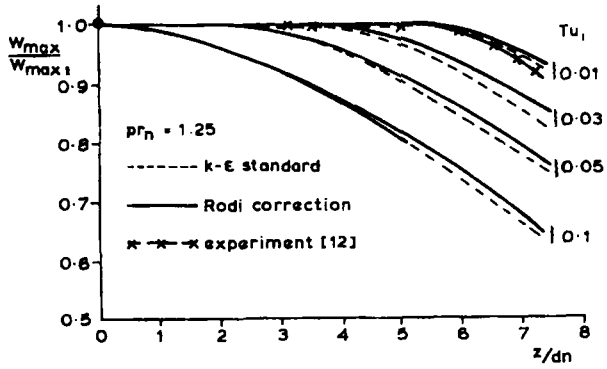


Figure 3. Subsonic free jet axial velocity decay

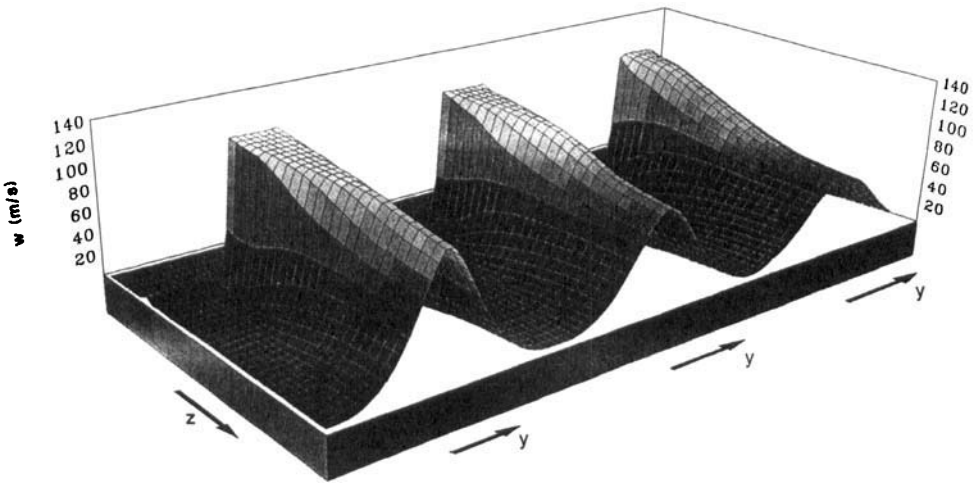


Figure 4. Comparison of subsonic free jet velocity profiles at pressure ratio of 1·1 and $Tu_1 = 1{\cdot}5$ per cent (left), 5 per cent (middle) and 15 per cent (right) with uniform nozzle exit velocity profile

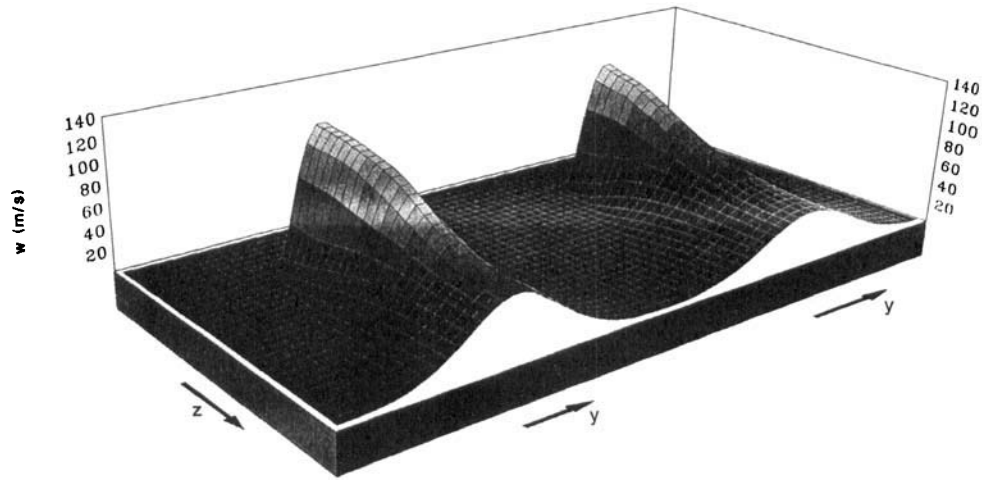


Figure 5. Subsonic free jet velocity profiles with parabolic nozzle exit velocity profile; $pr_n = 1{\cdot}1$, $Tu_1 = 1{\cdot}5$ per cent (left) and 5 per cent (right)

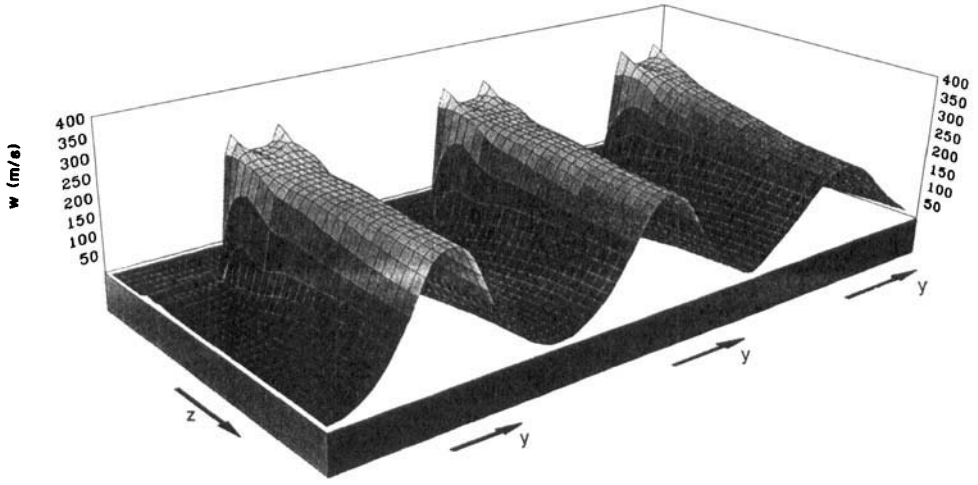


Figure 6. Supersonic free jet velocity profiles with uniform nozzle exit velocity profile; $pr_n = 2{\cdot}5$, $Tu_1 = 1{\cdot}5$ per cent (left), 5 per cent (middle) and 15 per cent (right)

based on the SIMPLE procedure used in PHOENICS. The predicted results were compared with the experiments of Curtis[13] and Poreh *et al.*[14] The implementation of the Rodi[9] and Malin[10] corrections for the constants used with the $k$–$\varepsilon$ model was in general similar to that used by Glynn and Jal.[2] In a small region very close to the impingement zone no corrections were applied, while in the free jet the Rodi correction was used and away from the impinging jet the Malin correction was used. Calculations were also performed with the Malin correction applied to both the wall jet and the free jet.

The predicted spread of the wall jet using various versions of the $k$–$\varepsilon$ model for $h/d_n = 7{\cdot}5$ is shown in Figure 9 compared with the experimental results of Poreh *et al.*[14] The four computational curves represent the predicted growth of the radial wall jet using respectively: the standard $k$–$\varepsilon$ model for both the free and wall jets; the Rodi correction for the free jet with the standard model for the wall jet; the

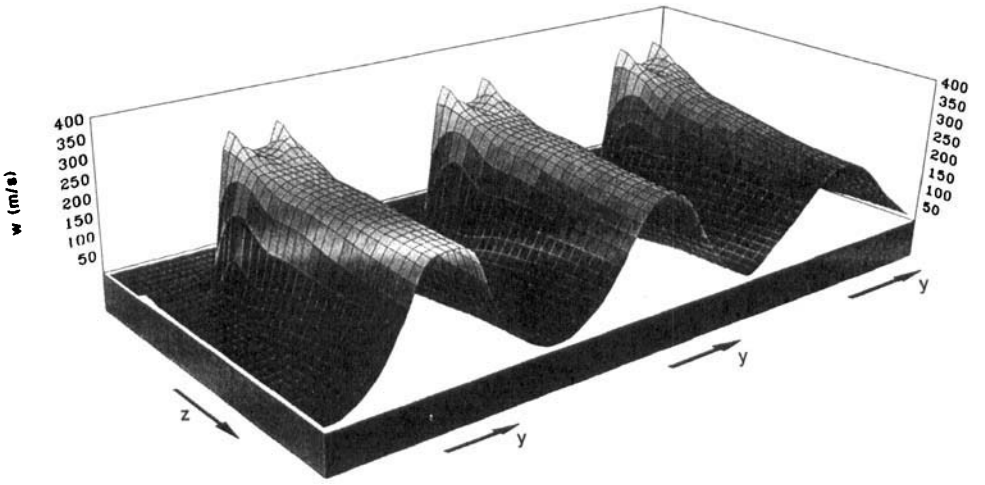


Figure 7. Supersonic free jet velocity profiles with uniform nozzle exit velocity profile; $pr_n = 3$, $Tu_1 = 1{\cdot}5$ per cent, 5 per cent (middle) and 15 per cent (right)

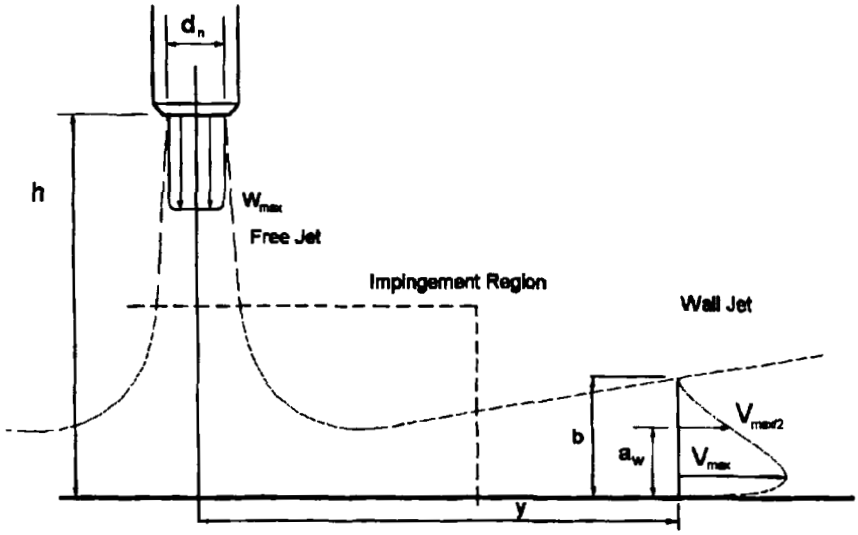


Figure 8. Characteristics of impinging jet flow field

standard model for the free jet with the Malin correction for the wall jet; and the Rodi correction for the free jet with the Malin correction for the wall jet. As observed by Knowles and Bray,[5] the standard $k$–$\varepsilon$ model underpredicts the spreading rate of the wall jet. Applying the Rodi correction to the free jet does not seem to change the spreading rate of the wall jet, but shifts its apparent origin. Thus wall jet predictions with the more accurately predicted free jet are actually worse in terms of thickness ($a_w$) at a given radial position ($y$).

Adding the Malin correction to the wall jet increases its spreading rate, as intended. The improvement, however, is only slight. Combining the Malin and Rodi corrections improves the 'Rodi only' results by increasing the wall jet spreading rate, but the initial thickness is still too low. Again, wall jet calculations with the more accurately predicted free jet are actually worse than with the standard $k$–$\varepsilon$ results for the free jet.

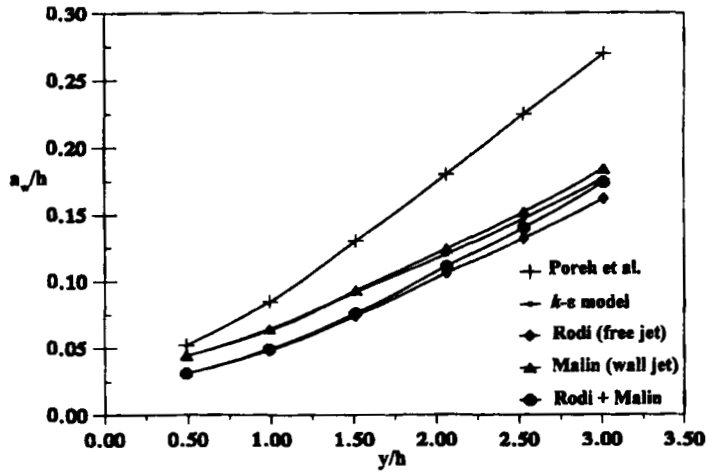


Figure 9. Effect of modified turbulence models on wall jet spreading

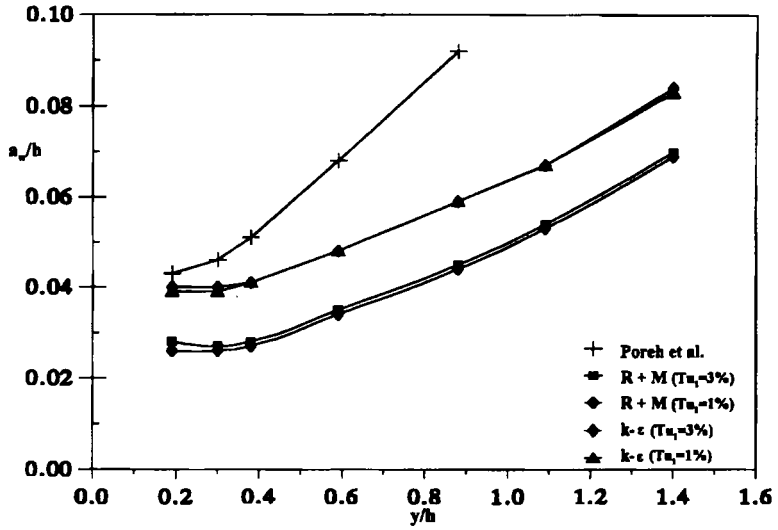


Figure 10. Effect of turbulence intensity on wall jet spreading—results using standard $k$–$\varepsilon$ model and Rodi + Malin corrections

There are seen to be two areas of error in the wall jet calculations. One is the predicted decay rate. This has been addressed by Malin,[10] who ascribes the failure of the standard $k$–$\varepsilon$ model in radial wall jets to an underestimation of the increased turbulent length scale (compared with the planar case). This increased length scale in turn is due to lateral divergence of the flow, which is present in the radial case but not in the round or planar cases. Bradshaw[15] has identified the surprisingly large effect of lateral divergence on turbulence structure. The other source of error is in the initial thickness of the wall jet. In our calculations this is seen to have a far greater effect on the predicted wall jet thickness than has the spreading rate itself.

It is worth noting that Figure 9 is showing the far-field behaviour of the wall jet to beyond $20d_n$ from the impingement point. By contrast, Glynn and Jal[2] placed their radial boundary at $12d_n$. Not only did

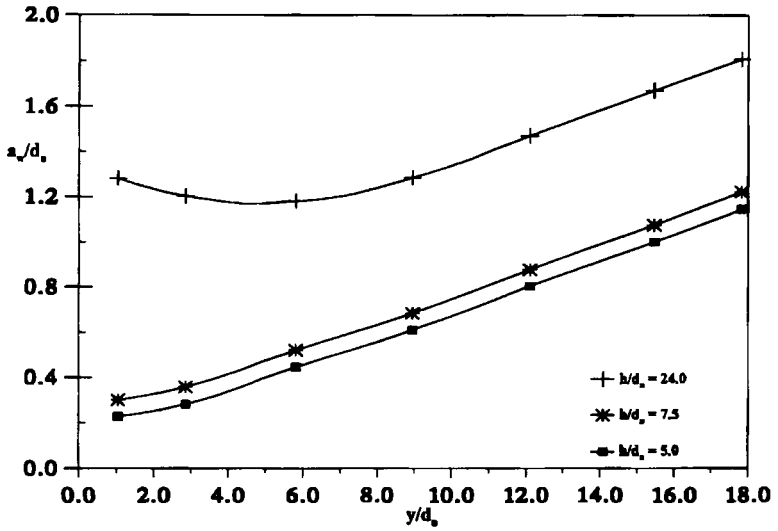


Figure 11. Effect of nozzle height on wall jet spreading using standard $k$–$\varepsilon$ turbulence model

this limit the range over which they could make comparisons with experiments, but the proximity of the boundary also seemed to affect some of their results, as discussed by Knowles and Bray.[5] The large radial extent of the present computations must be considered if V/STOL aircraft flows are to be modelled.[3]

The effect of nozzle exit turbulence intensity on the prediction of the wall jet thickness using the modified and unmodified versions of the $k$–$\varepsilon$ turbulence model seems to be negligible when $h/d_n = 7{\cdot}5$, as seen in Figure 10. This is not the case for the free jet, which has been found to be very much affected by the turbulence intensity at the jet exit when either version of the turbulence model is used. There *is* a small effect of nozzle exit turbulence level seen in Figure 10, but it is limited to a small change in initial wall jet thickness. Figure 11 shows the prediction of the wall jet spreading for various values of $h/d_n$. It can be seen from the figure that as $h/d_n$ increases, the wall jet thickness is increased. This tends to agree with some of our own recent measurements.[16]

## 4. CONCLUSIONS

A numerical study has been conducted using various versions of the $k$–$\varepsilon$ turbulence model to predict the hydrodynamic field of free and impinging jets. The effect on the flow field of nozzle pressure ratio, turbulence intensity, velocity profile and height above the ground were investigated. The following conclusions have been drawn.

(i) Increasing nozzle pressure ratio tends to reduce the free jet centreline velocity decay rate.
(ii) Increasing nozzle exit turbulence intensity promotes more rapid mixing and hence decay of the free jet. There is, however, a negligible effect on wall jet growth, confined to a small change in wall jet initial thickness.
(iii) Assuming a parabolic nozzle exit velocity profile rather than a uniform profile gives an increase in free jet decay.
(iv) Increasing the nozzle height was found to increase the wall jet thickness at a given radius. The decay rate, however, does not seem to be affected and the main influence seems to be through an increase in the initial wall jet thickness.
(v) The standard $k$–$\varepsilon$ model overpredicts the spreading rate of a free jet and underpredicts the spreading rate of a radial wall jet. The Rodi correction improves the free jet prediction and the Malin correction makes a small but inadequate improvement in the prediction of the radial wall jet.
(vi) The wall jet prediction is seen to be strongly dependent on the free jet calculation. A more accurate free jet calculation does not, however, necessarily produce a more accurate wall jet prediction; indeed, the opposite has been found to be the case in these calculations.

ACKNOWLEDGEMENTS

The computational results presented here were obtained by L. Bateup, M. Myszko and Dr. B. A. Jubran. Dr. D. Bray provided assistance in setting up the initial calculations. The support of the University of Jordan and RMCS during Dr. Jubran's sabbatical year at Shrivenham are acknowledged. This work was also part of a collaborative programme with the Instituto Superior Técnico, Lisbon. The support of the British Council, under the Treaty of Windsor programme, is gratefully acknowledged.

## APPENDIX: NOMENCLATURE

| | |
|---|---|
| $a_w$ | wall jet thickness to half peak velocity |
| $b$ | free jet or wall jet thickness |
| $c_p$ | specific heat at constant pressure |
| $c_D$ | turbulence model constant |
| $c_{1\varepsilon}$ | turbulence model constant |
| $c_{2\varepsilon}$ | turbulence model constant |
| $c_\mu$ | turbulence model constant |
| $d_n$ | diameter of nozzle |
| $f$ | mean flow retardation parameter (equation (10)) |
| $h$ | perpendicular height of nozzle exit above ground, or specific enthalpy (equation (15)) |
| $k$ | turbulent kinetic energy |
| $p$ | pressure |
| $pr_n$ | nozzle pressure ratio, $p_0/p_\infty$ |
| $r$ | radius of jet |
| $r_5$ | radius at which jet velocity equals $0{\cdot}5W_{max}$ |
| $R$ | specific gas constant |
| $S_\phi$ | source of $\phi$ per unit volume |
| $T$ | temperature |
| $Tu$ | turbulence intensity |
| $U$ | $x$-axis velocity |
| $V$ | $y$-axis velocity |
| $V_\tau$ | friction velocity |
| $V^+$ | dimensionless near-wall velocity |
| $W$ | $z$-axis velocity |
| $W_{max}$ | maximum jet velocity |
| $x$ | angular dimension in polar co-ordinate system |
| $y$ | horizontal (radial) distance |
| $z$ | vertical distance (measured in direction of jet flow from nozzle exit) |
| $z^+$ | dimensionless wall distance |

*Greek letters*

| | |
|---|---|
| $\varepsilon$ | rate of dissipation of turbulent kinetic energy |
| $\nu_l$ | laminar kinematic viscosity |
| $\nu_t$ | turbulent (eddy) kinematic viscosity |
| $\rho$ | density |

*Subscripts*

| | |
|---|---|
| 0 | stagnation |
| 1 | jet exit conditions |
| n | nozzle properties |
| w | wall jet properties |
| $\infty$ | ambient (cross-flow) |

## REFERENCES


1. P. E. Colin and D. Olivari, 'The impingement of a circular jet normal to a flat surface with and without cross-flow", *Euro. Research Office Rep. AD688-953*, 1969.
2. D. R. Glynn and E. N. Jal, 'Numerical prediction of flow in free and impinging jets', *CHAM Rep. 3181/1*, 1987.
3. K. Knowles and D. Bray, 'Recent research into the aerodynamics of ASTOVL aircraft in ground environment', *Proc. IMechE Pt. G: J. Aerosp. Eng.*, **205**, 123–131 (1991).
4. B. E. Launder, oral contribution to *SERC CFD Community Club Workshop 'Turbulence Modelling for Impinging Flow'*, Manchester, October 1991.
5. K. Knowles and D. Bray, 'Computation of normal impinging jets in cross-flow and comparison with experiment', *Int. j. numer. methods fluids*, **13**, 1225–1233 (1991).
6. W. P. Jones and J. J. McGuirk, 'Computation of a round turbulent jet discharging into a confined cross-flow', in *Turbulent Shear Flows 2*, Springer, Berlin, 1980, pp. 233–245.
7. R. E. Childs and D. Nixon, 'Turbulence and fluid/acoustic interaction in impinging jets', *Int. Powered Lift Conf.*, Santa Clara, CA, December 1987/S.A.E, Paper 872345.
8. J. M. Barata, D. F. G. Durao and J. J. McGuirk, 'Numerical study of a single impinging jet through a cross-flow', *AIAA J. Aircraft*, **26**, 1002–1007 (1989).
9. W. Rodi, *Turbulence Models and Their Application in Hydraulics—A State of the Art Review*, IAHR, Delft, 1980.
10. M. R. Malin, 'Prediction of radially spreading turbulent jets', *AIAA J.*, **26**, 750–752 (1988).
11. W. R. Van Dalsem, A. G. Panaras and J. L. Steger, 'Numerical investigation of a jet in ground effect with a cross-flow', *Int. Powered Lift Conf.*, Santa Clara, CA, December 1987/S.A.E., Paper 872344.
12. C. P. Donaldson and R. S. Snedeker, 'A study of free jet impingement, Part 1. Mean properties of free and impinging jets', *J. Fluid Mech.*, **45**, 281–319 (1971).
13. P. Curtis, 'Investigation into the behaviour of a single free jet in free air and impinging perpendicularly on the ground', *British Aerospace Rep. BAe-KAD-R-RES-3349*, 1987.
14. M. Poreh, Y. G. Tseui and J. E. Cermak, 'Investigation of a turbulent radial wall jet', *J. Appl. Mech.*, **89**, 457–472 (1967).
15. P. Bradshaw, 'Effects of streamline curvature on turbulent flow', *AGARDograph 169*, 1973.
16. K. Knowles and M. Myszko, 'Studies of impinging jet flows and radial wall jets', *Proc. Int. Symp. on Turbulence, Heat and Mass Transfer*, Lisbon, August 1994, pp. 2.1.1–2.1.6. (See also 'Turbulence, heat and mass transfer', eds. J. C. F. Pereira and K. Hanjalić, pp. 250–257, Begell House Inc., New York, 1996.)